Research article

Tingting Lv[a], Xieyu Chen[a], Guohua Dong, Meng Liu, Dongming Liu, Chunmei Ouyang*, Zheng Zhu, Yuxiang Li, Chunying Guan, Jiaguang Han, Weili Zhang, Shuang Zhang* and Jinhui Shi*

Dual-band dichroic asymmetric transmission of linearly polarized waves in terahertz chiral metamaterial

https://doi.org/10.1515/nanoph-2019-0507
Received December 7, 2019; revised January 12, 2020; accepted January 28, 2020

Abstract: Polarization conversion dichroism is of particular interest in manipulating the polarization state of light, whereas high-performance asymmetric transmission (AT) of linearly polarized waves is still inaccessible in the terahertz range. Here, a bilayer chiral metamaterial consisting of orthogonally chained S-shaped patterns with broken symmetry along the light propagation direction is proposed and demonstrated experimentally to realize a dual-band dichroic AT effect for linearly polarized terahertz waves. The AT effects are robust across a wide range of incident angles. The observed strong AT can be theoretically explained by a multiple reflection and transmission interference model and the transfer matrix method. The proposed bilayer chiral metamaterial may have broad applications in polarization manipulation, chiral biosensing and direction-dependent information processing.

Keywords: asymmetric transmission; chiral metamaterial; dichroic devices; THz applications.

1 Introduction

Over the past decades, many attempts have been devoted to manipulating the polarization, phase, amplitude and propagation direction of electromagnetic waves using metamaterials [1–9], exploiting their flexible structural designs and potential for compact integrated optical components. Meanwhile, various intriguing phenomena have been reported in metamaterials, including anomalous refraction [4, 5], invisibility [6], ideal Weyl point and surface state [7], optical activity [8, 9], and asymmetric transmission (AT) [10, 11]. Conventional methods such as the Faraday media can generate a nonreciprocal one-way effect by breaking the time-reversal symmetry with the aid of a static magnetic field. However, the presence of a static magnetic field prevents miniaturization and integration of photonic devices. To circumvent this, Fedotov et al. [10] proposed to achieve an AT effect for circularly polarized waves in an intrinsically 2D chiral metamaterial, which belongs to a family of reciprocal systems. The AT phenomenon in a lossy metamaterial refers to the difference in the total transmission intensity between forward and backward propagation directions for linearly or circularly polarized waves. The AT effect arises from different polarization conversion efficiencies along two opposite propagation directions. The AT effects can also be found in planar photonic metamaterial [12, 13], single plasmonic

[a]**Tingting Lv and Xieyu Chen:** These authors equally contributed to this work.
***Corresponding authors: Chunmei Ouyang,** Center for Terahertz Waves and College of Precision Instrument and Optoelectronics Engineering, Key Laboratory of Opto-electronics Information and Technical Science, Ministry of Education, Tianjin University, Tianjin 300072, China, e-mail: cmouyang@tju.edu.cn; **Shuang Zhang,** School of Physics and Astronomy, University of Birmingham, Birmingham B15 2TT, UK, e-mail: s.zhang@bham.ac.uk; and **Jinhui Shi,** Key Laboratory of In-Fiber Integrated Optics of Ministry of Education, College of Science, Harbin Engineering University, Harbin 150001, China, e-mail: shijinhui@hrbeu.edu.cn. https://orcid.org/0000-0002-7701-8247
Tingting Lv: Key Laboratory of In-Fiber Integrated Optics of Ministry of Education, College of Science, Harbin Engineering University, Harbin 150001, China; and School of Electronic Science, Northeast Petroleum University, Daqing 163318, China
Xieyu Chen, Meng Liu, Jiaguang Han and Weili Zhang: Center for Terahertz Waves and College of Precision Instrument and Optoelectronics Engineering, Key Laboratory of Opto-electronics Information and Technical Science, Ministry of Education, Tianjin University, Tianjin 300072, China
Guohua Dong, Zheng Zhu, Yuxiang Li and Chunying Guan: Key Laboratory of In-Fiber Integrated Optics of Ministry of Education, College of Science, Harbin Engineering University, Harbin 150001, China
Dongming Liu: School of Electronic Science, Northeast Petroleum University, Daqing 163318, China

Published online February 21, 2020

nanostructures [14], achiral metamaterial showing extrinsic 2D chirality at oblique incidence [15] and multilayer structures [16]. Drawing inspiration from the abovementioned works, the AT effects for both circularly [16–23] and linearly [24–32] polarized waves have been extensively reported. Among these, dual-band and active AT effects have attracted much interest [18–20, 31, 32]. Most of them are composed of multilayer coupled resonators with a few exceptions of single layer structures [17, 20]. These findings show that multilayer chiral metamaterials can greatly increase the polarization conversion and consequently enhance the AT effects. In particular, introducing symmetry breaking along the propagation direction has been regarded as a prerequisite in pursuit of the AT behavior of linear polarized waves [11, 29].

Following the initial experimental demonstration of the circular AT effect at ~11 GHz [10], the AT phenomena in terahertz metamaterials have also received much attention [33–40]. Although many efforts have been made to improve the performance of the AT effects, there are still some limitations including single polarization conversion, ultra-narrow bandwidth and low AT efficiency, which have not yet been addressed simultaneously [33–40]. In addition, complex structures or auxiliary grating layers in some designs hamper flexibility and robustness of the AT applications [35, 36, 39]. For instance, numerical studies showed that bilayer E-shaped metamaterial with embedded VO_2 could exhibit a tunable AT phenomenon for linear polarized waves in the THz regime, but they are not broadband and suffer from a single polarization conversion [34]. While polarization functional devices are key components for the prosperous progress of THz photonics and THz technologies, existing THz metamaterials are not compatible with high efficiency, broadband and dichroic polarization manipulation in practical applications. Therefore, it is of great significance to investigate and realize high-performance THz polarization devices exhibiting an AT phenomenon.

In this work, we theoretically and experimentally demonstrated dual-band dichroic AT of linearly polarized waves in terahertz chiral metamaterial. The proposed chiral metamaterial consists of twisted S-shaped patterns with symmetry broken along the light propagation direction. The orthogonal arrangement between the two layers gives rise to a strong coupling between orthogonal linearly polarized states in two separated frequency bands. It is worth mentioning that the so-called dichroic AT effects are robust within a wide angle of incidence up to 60° and suitable for manipulating different linearly polarized waves. The multiple reflection and transmission interference model and the transfer matrix method (TMM) provide theoretical explanations to the enhanced AT properties. In comparison with previously reported metamaterials, S-shaped chiral metamaterial offers an opportunity to realize high-efficiency dichroic nanophotonic devices with a wide range of potential applications in optical polarization manipulation, chiral biosensing and polarization information processing.

2 Results and discussion

Dichroic devices such as dichroic beamsplitters, filters and mirrors are widely used for controlling transmission and reflection of light as a function of wavelength in optical systems. Metamaterials have been utilized to realize dichroic polarization devices in the microwave regime [41, 42], but dichroic polarization manipulation is more desirable and significant in THz and optical ranges. An S-shaped metallic resonator, as a typical building block of metamaterial, has been investigated to accomplish enhanced polarization rotation, broadband bandpass filter and weak circular polarization conversion. Here, S-shaped metallic resonators are used to construct a chiral metamaterial showing a high-efficiency dichroic polarization effect. The proposed freestanding metamaterial configuration is schematically illustrated in Figure 1. A polyimide film with the thickness of $t = 24$ μm is embedded between the bilayer S-shaped aluminum resonators. The S-shaped metallic resonators in the front and back layers are identical in all structural parameters except that the back layer is mirrored along the x axis and then twisted by 90° around the z axis with respect to the front one. Furthermore, two additional polyimide layers with the same thickness of $t_1 = 10$ μm are coated on both sides of the metamaterial to protect the S-shaped resonators from the external environment. Each metamaterial layer seems to be chained S-shaped resonators that are made from $t_m = 200$ nm thick aluminum. Each unit cell is equivalent to a combination of an L-shaped resonator with an asymmetrical U-shaped resonator, with dimensions of $w = 10$ μm, $g_1 = 10$ μm and $g_2 = 10$ μm, as shown in Figure 1B. Conventional photolithography is employed to fabricate the metamaterial sample, which consists of 300×300 unit cells with a square period of $a = 60$ μm. The optical microscope image of the fabricated sample is shown in Figure 1C.

The dual-band dichroic polarization effect of S-shaped chiral metamaterial is verified theoretically, numerically and experimentally. Firstly, the THz responses of the metamaterial are investigated by performing 3D full-wave numerical simulations (CST Microwave Studio, Dassault Systèmes, Paris, France) with periodic boundary

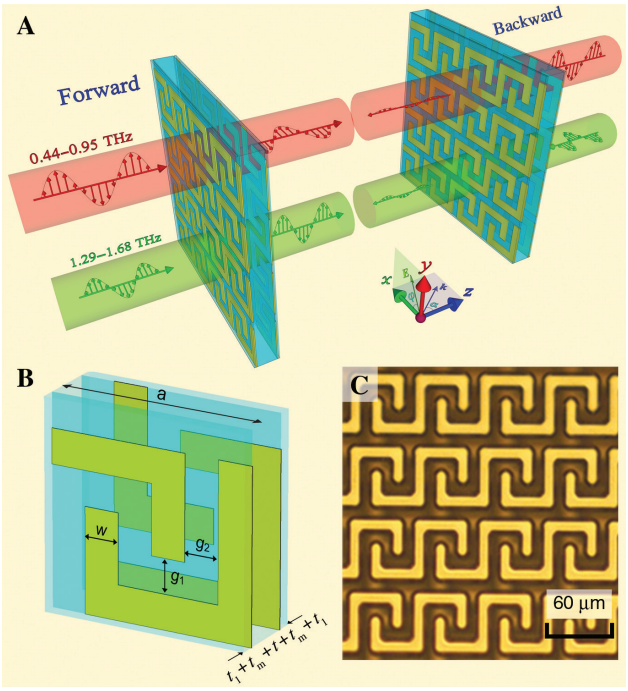

Figure 1: Structure and schematics of asymmetric transmission effect.
(A) Artistic rendering of the dichroic asymmetric transmission for the proposed chiral metamaterial. The normally forward incident *x* and *y* polarized waves can be transmitted and converted into their cross-polarization in two adjacent frequency bands, whereas they are blocked in the reversed direction. The polarization angle φ and incident angle α are marked in the inset. (B) Stereogram of a unit cell in the proposed metamaterial. Two 90° twisted and mirrored chained S-shaped aluminum layers are separated by a polyimide layer. (C) Optical microscope image of the fabricated sample.

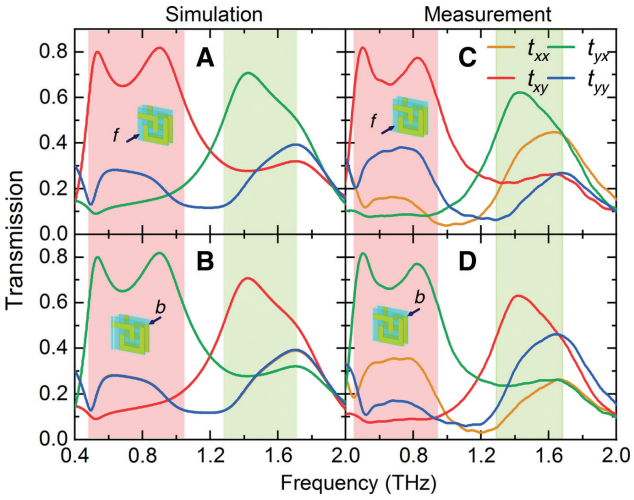

Figure 2: The results of simulation and measurement. Simulated (A), (B) and measured (C), (D) spectra of the four transmission coefficients along the forward (A), (C) and backward (B), (D) propagations. Curves t_{xx} and t_{yy} are completely identical in Figure 2A and B.

conditions along both *x* and *y* directions, to be consistent with the THz-time-domain spectroscopy (TDS) experiment. Here, a lossy metal model of aluminum is adopted with a conductivity of 3.56×10^7 S/m, and the polyimide layers can be treated as a lossy dielectric with $\varepsilon_p = 3 + 0.09\mathrm{i}$. The calculated transmission coefficients are denoted as T_{ij}^d in terms of Jones matrix $\left(t_{ij}^d = \left|T_{ij}^d\right|\right)$. The subscripts *i* and *j* correspond to the polarization states of the transmitted and incident waves, which could be either *x* or *y* linearly polarized waves in our case. The superscript *d* refers to forward (*f*, along the +*z* axis) or backward (*b*, along the −*z* axis) wave propagations. The transmission spectra are illustrated in Figure 2A, B for forward (+*z*) and backward (−*z*) propagating waves at normal incidence. One can conclude that the co-polarized transmission coefficients (t_{xx} and t_{yy}) are equal due to the structural rotational symmetry and the off-diagonal transmission coefficients interchange with each other along the opposite propagation directions based on the reciprocity theorem [43]. The cross-polarization coefficient t_{xy}^f has two remarkable resonant peaks with maxima of $t_{xy}^f = 0.80$ and 0.82 at 0.53 and 0.90 THz, respectively, which shows a full width half maximum (FWHM) bandwidth of 0.57 THz. Likewise, the curve of t_{yx}^f exhibits a maximum of 0.71 near the resonance at 1.42 THz with the FWHM bandwidth of 0.43 THz. In addition, the magnitudes of the co-polarization coefficients are small, ranging between 0.1 and 0.3 across the whole investigated frequency band. For *x*- and *y*-polarized wave incidence, the resonant absorption limits the transmission efficiency. Choosing a low loss substrate may improve the cross-polarization conversion ratio.

The experimental characterization is performed by utilizing a broadband (0.2–4 THz) THz-TDS with an 8-F confocal collimation system. A normally incident linear polarized terahertz beam is focused to a spot with an approximate 5 mm diameter and illuminated onto the center of the 18×18 mm^2 metamaterial sample. The measured transmission coefficient T_m of the S-shaped metamaterial is extracted by taking the ratio between the measured sample transmission spectrum E_{sample} and the referenced transmission spectrum $E_{reference}$ without the metamaterial sample, such that $T_m = E_{sample}/E_{reference}$, as shown in Figure 2C, D. The measurement data of the cross-polarization transmission coefficients t_{xy} and t_{yx} are in good agreement with the simulation ones. However, there is a noticeable difference between the amplitudes of t_{xx} and t_{yy}, which may arise from the dimension deviations and misalignment of the bilayer metamaterial in the sample fabrication. These results reveal that the proposed metamaterial has a pronounced dual-band cross-polarization conversion and dichroic polarization manipulation.

The AT response is usually characterized by the difference of transmission between forward and backward propagation for an incident beam of fixed polarization state [43].

$$\begin{aligned}\Delta^x &= |T_{xx}^f|^2 + |T_{yx}^f|^2 - |T_{xx}^b|^2 - |T_{yx}^b|^2 \\ \Delta^y &= |T_{yy}^f|^2 + |T_{xy}^f|^2 - |T_{yy}^b|^2 - |T_{xy}^b|^2 = -\Delta^x\end{aligned} \tag{1}$$

These simulated and measured AT parameters Δ^x and Δ^y for forward propagating waves are exhibited in Figure 3A. Apparently, they are exactly opposite to each other. It can be clearly seen that a pronounced dichroic AT response is demonstrated in the proposed S-shaped metamaterial, where two resonant peaks in the lower frequency band confirm that the metamaterial allows forward *y* polarized waves to pass through, while it prevents the forward propagation of *x* polarized waves. In the higher frequency band, the AT is exactly reversed, with a higher transmission of forward *x* polarized waves than that of forward *y* polarized waves. In the experiment, the AT parameter Δ^y reaches maxima of 0.73 and 0.71 at around 0.51 and 0.82 THz, respectively, and Δ^x reaches a maximum of 0.45 at around 1.44 THz. The simulation and measured AT results agree well with each other. Further numerical simulations reveal that the dichroic AT property is robust against the change of incident angles α (see Figure 1A), maintaining a high efficiency over a wide range of incident angles up to 60°, as shown in Figure 3B. The dichroic AT effect is also suitable for a wide incident polarization angle φ. Interestingly, the AT effect between 0–45° and 45–90° polarization angles satisfies an antisymmetric property with respect to 45°, while it vanishes when the polarization angle is close to 45°, as shown in Figure 3C. The absence of the AT can be attributed to a particular symmetry, where the bilayer S-shaped metamaterial structure has two-fold rotational symmetry along an axis aligned to a 45° polarization angle.

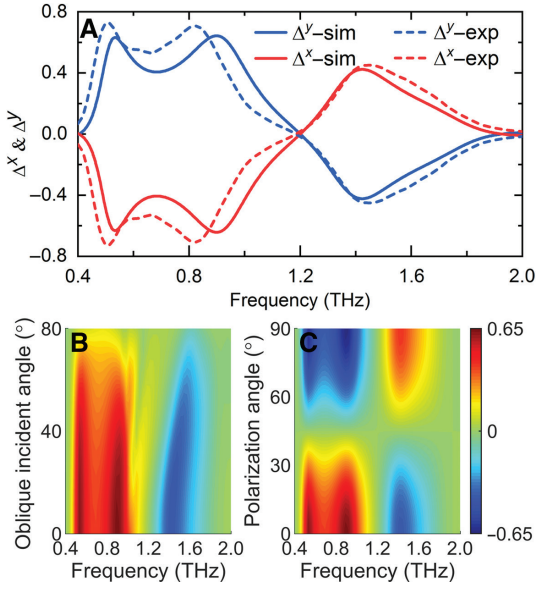

Figure 3: Analysis of asymmetric transmission properties. (A) Simulated and measured asymmetric transmission parameters along the forward propagation. Simulated asymmetric transmission of the metamaterial as a function of (B) incident angle α and (C) polarization angle φ, in which only one parameter is variable and the others are kept unchanged.

In order to elucidate the enhanced dichroic AT properties and polarization coupling mechanism, a multiple reflection and transmission interference model is employed, which takes into account the air-polyimide interface and the two S-shaped resonator layers, as depicted in Figure 4A, in which the S-shaped arrays are treated as zero thickness impedance-tuned surfaces. This model neglects the near field coupling between the interfaces. To implement this concept, we employ a 4×4 TMM based on reflection and transmission coefficients on each side of the interface. Generally, for a planar metamaterial structure between two boundary media *a* and *b*, the 4×4 transfer matrix M_{ba} can be expressed in terms of the forward and backward propagating fields [44]:

$$(E_{bx}^f, E_{by}^f, E_{bx}^b, E_{by}^b)^T = M_{ba}(E_{ax}^f, E_{ay}^f, E_{ax}^b, E_{ay}^b)^T \tag{2}$$

For a multilayer metamaterial composed of several interfaces, the overall transfer matrix *M* is expressed as a multiplication of the transfer matrices of each individual interface:

$$M = \begin{pmatrix} m_{11} & m_{12} \\ m_{21} & m_{22} \end{pmatrix} - \begin{pmatrix} m_{13} & m_{14} \\ m_{23} & m_{24} \end{pmatrix} \begin{pmatrix} m_{33} & m_{34} \\ m_{43} & m_{44} \end{pmatrix}^{-1} \begin{pmatrix} m_{31} & m_{32} \\ m_{41} & m_{42} \end{pmatrix} \tag{3}$$

where m_{mn} denotes the mth row and nth column element of the overall 4×4 transfer matrix *M*. Based on the TMM and numerical simulation, the calculated spectra of the cross-polarization transmission coefficients for forward propagation are presented in Figure 4B.

In order to characterize the polarization properties of the transmitted wave, the polarization rotation angle θ, the ellipticity angle η and circular dichroism (CD, referred to the difference in transmittance between right-handed circularly polarized and left-handed circularly polarized waves) are calculated as:

$$\begin{aligned}\theta &= -\frac{1}{2}[\arg(T_{++}) - \arg(T_{--})] \\ \eta &= \frac{1}{2}\arcsin\left(\frac{|T_{++}|^2 - |T_{--}|^2}{|T_{++}|^2 + |T_{--}|^2}\right) \\ \mathrm{CD} &= |T_{++}|^2 - |T_{--}|^2\end{aligned} \tag{4}$$

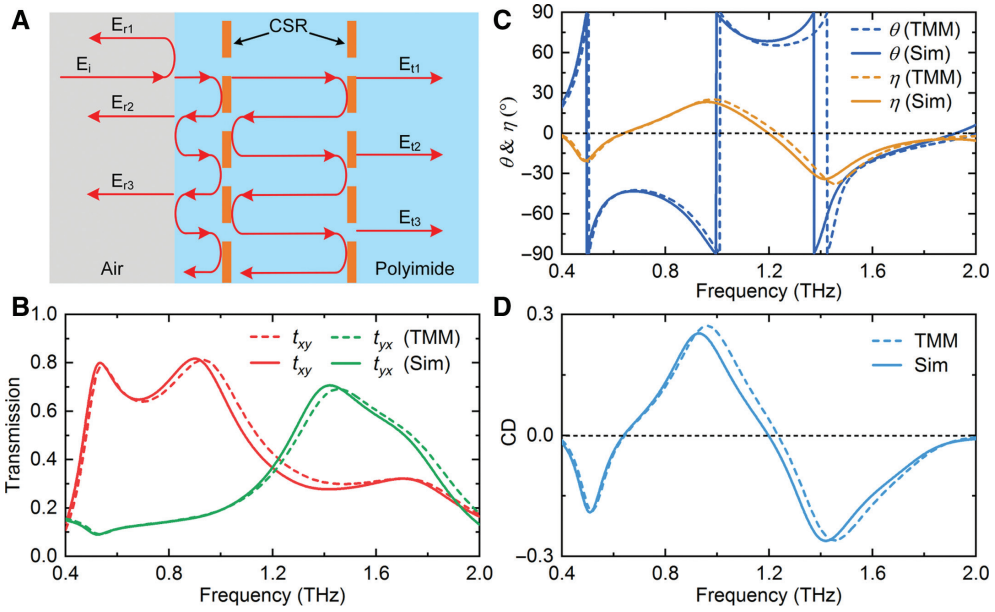

Figure 4: The theoretical analysis of the multiple reflection and transmission interference theory.
(A) Schematic of the multiple reflection and transmission interference model in the bilayer metamaterial with chained S-shaped resonators (CSR). (B) Theoretically calculated and numerically simulated cross-polarization transmission coefficients. (C) Polarization rotation azimuth angle θ and ellipticity η. (D) Circular dichroism.

where T_{++} and T_{--} are the transmission coefficients for right-handed circularly polarized and left-handed circularly polarized waves. The theoretical results and simulated data for these three parameters are shown in Figure 4C, D. It is noted that all the transmission fields are elliptically polarized at the three resonant frequencies since the ellipticity angle η is 14.9°, –21.4° and 34° at 0.53, 0.90 and 1.42 THz, respectively. In-between the resonant frequencies, the transmitted wave appears linearly polarized since η is close to 0 and the corresponding polarization rotation angle θ reaches –45° and 69° at the frequencies of 0.64 and 1.20 THz, respectively, indicating a strong optical activity. Furthermore, the proposed multilayer metamaterial exhibits 3D chirality, with the highest circular dichroism reaching 26% at around 1.42 THz. A large circular dichroism can be expected by the introduction of strong 3D chirality that leads to a large difference between two circularly polarized waves [45, 46]. Overall, there is an excellent agreement between the numerical and theoretical results, validating the use of a multiple reflections and transmissions interference model in understanding the multilayer metamaterial-light interaction and the enhanced dichroic AT phenomenon, despite the negligence of the near-field interaction between the layers. In order to gain insight into the physical mechanisms of the dichroic AT effect, the distributions of the Z-component magnetic field at the three resonances are presented. In the case of a normally incident y-polarized wave as shown in Figure 5A, B, the antisymmetric and

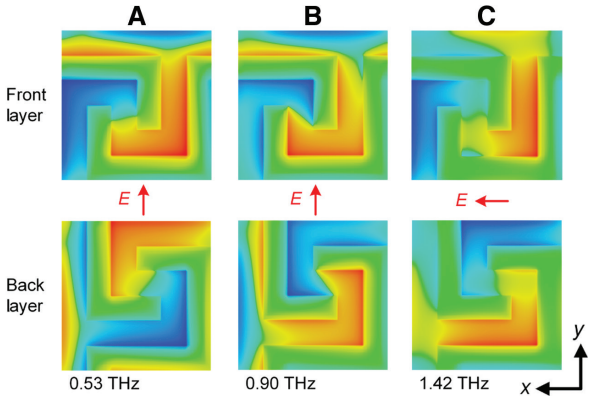

Figure 5: Z-component magnetic field distributions at three resonant asymmetric transmission (AT) peaks.
The resonant frequencies are (A) 0.53 THz, (B) 0.90 THz and (C) 1.42 THz.

symmetric modes are excited at 0.53 THz and 0.90 THz, respectively. In contrast, the symmetric mode dominates the AT effect at 1.42 THz for a normally incident *x*-polarized wave, as shown in Figure 5C.

To investigate the influence of structural parameters on the proposed AT properties, the cross-polarization transmission curves are investigated for three different vertical distances g_1 between L-shaped and asymmetrical U-shaped resonators. The simulated and measured results of the three cases are shown in Figure 6A, B. All resonant peaks are sensitive to the vertical distance g_1, and an appropriate distance enables a good AT performance with high efficiency and

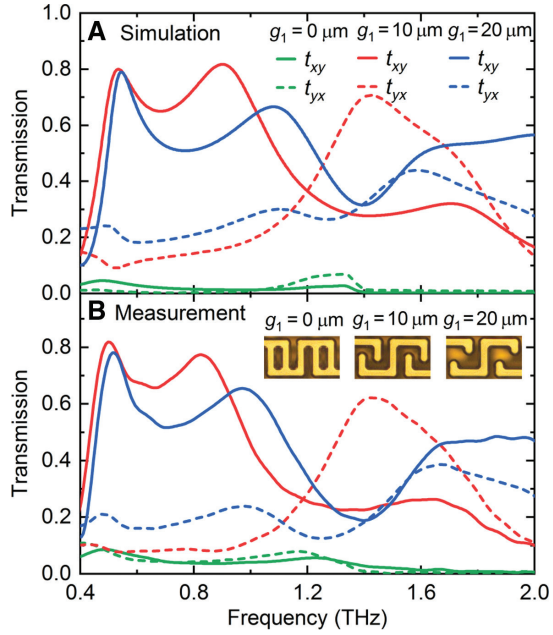

Figure 6: Cross-polarization transmission with different vertical distance g_1.
(A) simulation and (B) measurement.

broadband operation. For a monolayer S-shaped structure with a distance of $g_1 = 0$, the metamaterial does not show cross-polarization conversion, but it has an anisotropic response. The corresponding T matrix is given:

$$T_{\text{CSR\_up}} = \begin{bmatrix} t_{xx} & t_{xy} \\ t_{yx} & t_{yy} \end{bmatrix} \propto \begin{bmatrix} A & 0 \\ 0 & D \end{bmatrix} \tag{5}$$

The bottom layer structure is related to the top layer by rotating an angle of 90° with respect to the z axis, followed by another rotation of 180° with respect to the y axis. The T matrix of the bottom layer structure is shown:

$$T_{\text{CSR\_bottom}} = \begin{bmatrix} t_{xx} & t_{xy} \\ t_{yx} & t_{yy} \end{bmatrix} \propto \begin{bmatrix} -1 & 0 \\ 0 & 1 \end{bmatrix}^{-1} \begin{bmatrix} 0 & -1 \\ 1 & 0 \end{bmatrix}^{-1}$$
$$T_{\text{CSR\_up}} \begin{bmatrix} 0 & -1 \\ 1 & 0 \end{bmatrix} \begin{bmatrix} -1 & 0 \\ 0 & 1 \end{bmatrix} \propto \begin{bmatrix} D & 0 \\ 0 & A \end{bmatrix} \tag{6}$$

The T matrix of the layer-by-layer metamaterial is proportional to the product of the two matrices as shown:

$$T_{\text{CSR\_hybrid}} = \begin{bmatrix} t_{xx} & t_{xy} \\ t_{yx} & t_{yy} \end{bmatrix} \propto \begin{bmatrix} AD & 0 \\ 0 & DA \end{bmatrix} \tag{7}$$

Hence, the bilayer S-shaped structure with a simple rotation has no cross-polarization conversion according to the T matrix method [43, 47]. Remarkably, the vertical distance is an important parameter for realizing dual-band dichroic polarization manipulation and it controls the on and off of the dichroic cross-polarization conversion, which offers a practical approach to develop tunable AT of linearly polarized waves in polarization modulation applications.

3 Conclusion

In summary, we theoretically and experimentally demonstrate a dual-band dichroic AT for linearly polarized waves in S-shaped chiral metamaterial. The results indicate that a strong dichroic AT response can be implemented with a maximum of $\Delta^y = 0.73$ and $\Delta^x = 0.45$ along the forward direction. The broadband and high-efficiency AT properties are robust over a wide angle of incidence up to 60°. Meanwhile, the anisotropy and chirality of the metamaterial give rise to cross-polarization conversion with a ratio over 0.8 and an FWHM greater than 0.50 THz. The dual-band dichroic AT properties can be well understood based on the multiple reflection and transmission interference theory, and the concept is validated quantitatively through the 4×4 TMM. The proposed bilayer chiral metamaterials have potential applications in designing THz polarization devices for practical polarimetry applications.

Acknowledgements: This work was supported by the National Natural Science Foundation of China under Grant Nos. 61875044, 91750107, 61675054, 61420106006, partly by the Natural Science Foundation of Heilongjiang Province under Grant No. ZD2018015, 111 project to the Harbin Engineering University under Grant No. B13015, Fundamental Research Funds for the Central Universities. S.Z. would like to acknowledge support from ERC Consolidator Grant (Topological) and the Royal Society and Wolfson Foundation.

References

[1] Gansel JK, Thiel M, Rill MS, et al. Gold helix photonic metamaterial as broadband circular polarizer. Science 2009;325:1513–5.
[2] Scheuer J. Metasurfaces-based holography and beam shaping: engineering the phase profile of light. Nanophotonics 2017;6:137–52.
[3] Shi JH, Ma HF, Guan CY, Wang ZP, Cui TJ. Broadband chirality and asymmetric transmission in ultrathin 90°-twisted Babinet-inverted metasurfaces. Phys Rev B 2014;89:165128.
[4] Yu NF, Genevet P, AKats M, et al. Light propagation with phase discontinuities: generalized laws of reflection and refraction. Science 2011;334:333–7.

[5] Grady NK, Heyes JE, Chowdhury DR, et al. Terahertz metamaterials for linear polarization conversion and anomalous refraction. Science 2013;340:1304–7.
[6] Pendry JB, Luo Y, Zhao R. Transforming the optical landscape. Science 2015;348:521–4.
[7] Yang B, Guo Q, Tremain B, et al. Ideal Weyl points and helicoid surface states in artificial photonic crystal structures. Science 2018;359:1013–6.
[8] Decker M, Klein MW, Wegener M. Circular dichroism of planar chiral magnetic metamaterials. Opt Lett 2007;32:856–8.
[9] Zarifi D, Soleimani M, Nayyeri V. Dual- and multiband chiral metamaterial structures with strong optical activity and negative refraction index. IEEE Antennas Wireless Propag Lett 2012;11:334–7.
[10] Fedotov VA, Mladyonov PL, Prosvirnin SL, Rogacheva AV, Chen Y, Zheludev NI. Asymmetric propagation of electromagnetic waves through a planar chiral structure. Phys Rev Lett 2006;97:167401.
[11] Menzel C, Helgert C, Rockstuhl C, et al. Asymmetric transmission of linearly polarized light at optical metamaterials. Phys Rev Lett 2010;104:253902.
[12] Schwanecke AS, Fedotov VA, Khardikov VV, Prosvirnin SL, Chen Y, Zheludev NI. Nanostructured metal film with asymmetric optical transmission. Nano Lett 2008;8:2940–3.
[13] Plum E, Fedotov VA, Zheludev NI. Planar metamaterial with transmission and reflection that depend on the direction of incidence. Appl Phys Lett 2009;94:131901.
[14] Drezet A, Genet C, Laluet JY, Ebbesen TW. Optical chirality without optical activity: How surface plasmons give a twist to light. Opt Express 2008;16:12559–70.
[15] Plum E, Fedotov VA, Zheludev NI. Extrinsic electromagnetic chirality in metamaterials. J Opt A: Pure Appl Opt 2009;11:074009.
[16] Pfeiffer C, Zhang C, Ray V, Guo LJ, Gribic A. High performance bianisotropic metasurfaces: asymmetric transmission of light. Phys Rev Lett 2014;113:023902.
[17] Pan C, Ren M, Li Q, Fan S, Xu J. Broadband asymmetric transmission of optical waves from spiral plasmonic metamaterials. Appl Phys Lett 2014;104:121112.
[18] Tang DF, Wang C, Pan WK, Li MH, Dong JF. Broad dual-band asymmetric transmission of circular polarized waves in near-infrared communication band. Opt Express 2017;25:11329–39.
[19] Liu JY, Li ZC, Liu WW, Cheng H, Chen SQ, Tian JG. High-efficiency mutual dual-band asymmetric transmission of circularly polarized waves with few-layer anisotropic metasurfaces. Adv Opt Mater 2016;4:2028–34.
[20] Li ZC, Liu WW, Cheng H, Chen SQ, Tian JG. Tunable dual-band asymmetric transmission for circularly polarized waves with graphene planar chiral metasurfaces. Opt Lett 2016;41:3142–5.
[21] Wu L, Yang ZY, Cheng YZ, et al. Giant asymmetric transmission of circular polarization in layer-by-layer chiral metamaterials. Appl Phys Lett 2013;103:021903.
[22] Zhang F, Pu MB, Li X, et al. All-dielectric metasurfaces for simultaneous giant circular asymmetric transmission and wavefront shaping based on asymmetric photonic spin–orbit interactions. Adv Funct Mater 2017;27:1704295.
[23] Cao T, Li Y, Zhang XY, Zou Y. Theoretical study of tunable chirality from graphene integrated achiral metasurfaces. Photon Res 2017;5:441–9.
[24] Kang M, Chen J, Cui HX, Li Y, Wang HT. Asymmetric transmission for linearly polarized electromagnetic radiation. Opt Express 2011;19:8347–56.
[25] Han J, Li H, Fan Y, et al. An ultrathin twist-structure polarization transformer based on fish-scale metallic wires. Appl Phys Lett 2011;98:151908.
[26] Mutlu M, Akosman AE, Serebryannikov AE, Ozbay E. Diodelike Asymmetric transmission of linearly polarized waves using magnetoelectric coupling and electromagnetic wave tunneling. Phys Rev Lett 2012;108:213905.
[27] Huang C, Feng YJ, Zhao JM, Wang ZB, Jiang T. Asymmetric electromagnetic wave transmission of linear polarization via polarization conversion through chiral metamaterial structures. Phys Rev B 2012;85:195131.
[28] Zhang C, Pfeiffer C, Jang T, et al. Breaking Malus' law: highly efficient, broadband, and angular robust asymmetric light transmitting metasurface. Laser Photonics Rev 2016; 10:791–8.
[29] Kim M, Yao K, Yoon G, Kim I, Liu YM, Rho J. A broadband optical diode for linearly polarized light using symmetry-breaking metamaterials. Adv Opt Mater 2017;5:1700600.
[30] Wang YH, Jin RC, Li J, Li JQ, Dong ZG. Enhanced asymmetric transmissions attributed to the cavity coupling hybrid resonance in a continuous omega-shaped metamaterial. Opt Express 2018;26:3508–17.
[31] Wu LX, Zhang M, Zhu B, Zhao JM, Jiang T, Feng YJ. Dual-band asymmetric electromagnetic wave transmission for dual polarizations in chiral metamaterial structure. Appl Phys B 2014;117:527–31.
[32] Chen K, Feng YJ, Cui L, Zhao JM, Jiang T, Zhu B. Dynamic control of asymmetric electromagnetic wave transmission by active chiral metamaterial. Sci Rep 2017;7:42802.
[33] Singh R, Plum E, Menzel C, et al. Terahertz metamaterial with asymmetric transmission. Phys Rev B 2009;80:153104.
[34] Lv TT, Li YX, Ma HF, et al. Hybrid metamaterial switching for manipulating chirality based on VO2 phase transition. Sci Rep 2016;6:23186.
[35] Fan WJ, Wang YR, Zheng RQ, Liu DH, Shi JW. Broadband high efficiency asymmetric transmission of achiral metamaterials. Opt Express 2015;23:19535–41.
[36] Cheng YZ, Gong RZ, Wu L. Ultra-broadband linear polarization conversion via diode-like asymmetric transmission with composite metamaterial for terahertz waves. Plasmonics 2017;12:1113–20.
[37] Serebryannikov AE, Ozbay E, Nojima S. Asymmetric transmission of terahertz waves using polar dielectrics. Opt Express 2014;22:3075–88.
[38] Zhang S, Liu F, Zentgraf T, Li J. Interference-induced asymmetric transmission through a monolayer of anisotropic chiral metamolecules. Phys Rev A 2013;88:023823.
[39] Xu ST, Fan F, Chen M, Ji YY, Chang SJ. Terahertz polarization mode conversion in compound metasurface. Appl Phys Lett 2017;111:031107.
[40] Fang SY, Luan K, Ma HF, et al. Asymmetric transmission of linearly polarized waves in terahertz chiral metamaterials.J Appl Phys 2017;121:033103.
[41] Shi JH, Liu XC, Yu SW, et al. Dual-band asymmetric transmission of linear polarization in bilayered chiral metamaterial. Appl Phys Lett 2013;102:191905.

[42] Wu SZ, Xu S, Zinenko TL, Yachin VV, Prosvirnin SL, Tuz VR. 3D-printed chiral metasurface as a dichroic dual-band polarization converter. Opt Lett 2019;44:1056–9.
[43] Menzel C, Rockstuhl C, Lederer F. Advanced Jones calculus for the classification of periodic metamaterials. Phys Rev A 2010;82:053811.
[44] Chen HT, Zhou JF, O'Hara JF, Chen F, Azad AK, Taylor AJ. Antireflection coating using metamaterials and identification of its mechanism. Phys Rev Lett 2010;105:073901.
[45] Chen Y, Gao J, Yang XD. Chiral metamaterials of plasmonic slanted nanoapertures with symmetry breaking. Nano Lett 2019;8:1701–18.
[46] Chen Y, Yang XD, Gao J. 3D Janus plasmonic helical nanoapertures for polarization-encrypted data storage. Light Sci Appl 2019;8:45.
[47] Wang YK, Wen XJ, Qu Y, Wang L, Wan RG, Zhang ZY. Co-occurrence of circular dichroism and asymmetric transmission in twist nanoslit-nanorod arrays. Opt Express 2016;24:16425–33.